SMALLEST OCXO WITH 1.5US OVER 24H HOLDOVER FOR DEMANDING SYNCHRONIZATION APPLICATION

Gweltas BEAUTO, Jean-Charles BILLEBAULT, Rami KHOURI, Vincent CANDELIER
RAKON France SAS / 10, Avenue des Louvresses – Business Park « Carré-92 »
92230 GENNEVILLIERS – France

Email : vincent.candelier@rakon.com

***Abstract*— In this paper, performance of a new generation of small OCXOs (ROD2522S2) are presented. Measurements show a very low sensitivity of the output frequency to temperature variation in real condition and in different smart use cases (PPS DO & HV MOD). A maximum of 1.5us time deviation over 24h period of holdover is achieved for many different conditions. We also present the thermo-mechanical simulation method used for optimizing the design and compacting the OCXO thermal control structure . The integration of the ageing and temperature compensation with a microcontroller in the product was developed previously for other platforms. The ageing compensation can be done after a frequency ageing learning phase using the phase difference between a GNSS receiver 1pps signal and the OCXO 1pps output signal. It has a very small volume of 25x22x12mm^3, compared to the one of 38x27x12mm^3 of the previous model ROD3827. The platform dimensions and pin out are fully compatible with the current telecom infrastructure phase and frequency reference. The optimization of the thermostat was done using a finite-element thermo-mechanical simulation of the ROD2522S2 platform. The warm up simulation with an external temperature of -40°C gave all the temperature variations of the critical components for the dynamic response and the stabilized state. With a non-linear RF simulation, we found the impact of the critical components on the thermal frequency sensitivity. From these two results of simulation, the optimization of the design permitted to have a very small simulated thermal frequency sensitivity (<5E-10) and a very small, simulated hysteresis (1E-10/°C/min) in the temperature range -40°C to 85°C. The ROD2522S2 frequency versus temperature sensitivity measurement is shown and in all vertical orientations (X, Y, Z) of the product in the thermal chamber. The frequency hysteresis with a gradient of 1°C/min is very small (<+/- 5E-11). The holdover performance is shown for 7 devices of 1PPS disciplined OCXO (PPS DO) and in holdover module mode (HV MOD). HV MOD means the product is in free run during the learning phase of its frequency ageing and with an ageing compensation during the holdover period. In these two modes conditions and with a 40 °C cycle variation of temperature with a gradient of 10°C/h or one step of 4°C, the parts have a time interval error less than 1.5us over 24h of holdover.**

This platform, with a pending patent, is now in production and ready for demanding synchronization application.

Keywords—OCXO, holdover, thermal simulation.

I. INTRODUCTION

We have created a new generation of OCXO, the ROD2522S2, with a very low temperature sensitivity of its frequency and with different smart operational modes (PPS DO, HV MOD) to be fully compatible with the current telecom infrastructure phase and frequency reference package (Fig. 1). It can achieve a maximum of 1.5us time deviation over 24h period of holdover for many different conditions.

We present the thermo-mechanical simulation method we used for optimizing the design in this compact structure. The integration of the ageing and the temperature compensation with a microcontroller in the product was developed from the previous bigger products [1],[2]. We will compare the measurement and the simulation results of the frequency temperature sensitivity, the frequency hysteresis. The holdover performances will be shown in different conditions of temperature variation.

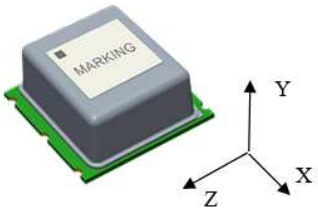

Fig. 1. ROD2522S2 (25*22*12 mm^3 SMD package).

II. THERMO-MECHANICAL SIMULATION METHOD

The parameters variation to reduce to have a good holdover performance during a temperature variation are the ageing, the ADEV, the temperature stability and the hysteresis, as shown in [1]. That's why it is very important to optimize the thermostat for that. The optimization of the thermostat was done using a finite element thermo-mechanical simulation of the ROD2522S2. A warm up simulation is created where a fixed heating power, P, is applied with an external temperature, Text, of -40°C. That gives all the temperature variations of the critical components requested for the dynamic response and the stabilized state (Fig.2). The critical components to stabilize in temperature are: the thermistor and the heater transistor of the thermal

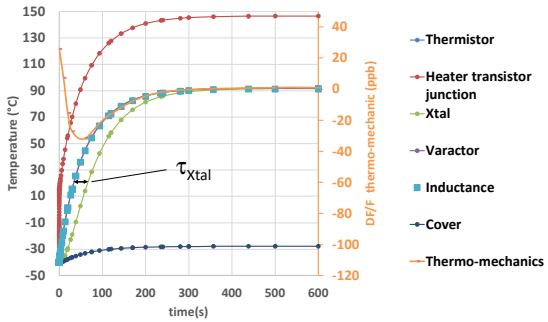

Fig. 2. ROD2522S2 warm up thermo-mechanical simulation: Temperature variation of the critical components and frequency variation due to thermo-mechanical constraints. t_{Xtal} delay between thermistor curve and Xtal curve.

regulation loop, the Xtal, the varactor, the inductor used in the oscillator and the constraints applied to the Xtal. From the warm up curves, we can extract for each component X, at each time t, its temperature difference versus the thermistor temperature, Tth, as reference, DTx(t), and its gain Gx(t) due to the thermostat. DTx(t) and Gx(t) are defined by:

$$DTx(t) = Tx(t) - Tth \ , \quad (1)$$

$$Gx(t) = DTx(t) / (Tx(t) - Text) \ . \quad (2)$$

At the final time (steady state), we have the temperature Tfx. DTfx and Gfx are also the maximum variation of temperature and the gain seen by the component X, when the external temperature describes -40°C to 85°C and when the thermistor temperature is continously stabilized by the thermal loop. We can also calculate the instantaneous temperature slope versus the time seen by each component, Stx(t), during the warm up. Then the temperature hysteresis, $Hys_T(t)$ is given by:

$$Hys_{Tx}(t) = (DTx(t) - DTxf) / Stx(t). \quad (3)$$

The maximum value of $Hys_{Tx}(t)$ defines the effective hysteresis Hys_{Tx} for the component X. During a temperature cycling -40°C to 85°C and when the thermistance temperature is regulated, the hysteresis Hys_{Tx} is multiplied by the gain Gxf. In this condition, the frequency hysteresis Hys_{Fx} and the final frequency variation DF/F_xf due to this component are:

$$Hys_{Fx} = Hys_{Tx} \ . \ SFx \ . \ Gxf \ , \quad (4)$$

$$DF/F_xf = SFx \ . \ DTxf \ . \quad (5)$$

where SFx is the OCXO frequency temperature sensitivity due to the component X. The impact of the critical components on the thermal frequency sensitivity, SFx, is found with a non-linear RF simulation of the oscillator frequency thermal sensitivity.

The thermal dilatation of the different parts of the structure gives constraints on the Xtal resonator. The 6 constraints, Ci, are simulated with the thermal load of all OCXO's components during the warm up at each temperature T_Q (t) and converted in frequency, $DF/F_C(t)$, with the frequency versus the constraint sensitivity of the resonator, k_i, [7], [8]:

$$DF/F_C(t) = \sum_{i=1}^{6} k_i \ C_i(t) \ . \quad (6)$$

The final value of the $DF/F_C(t)$, DF/F_Cf, is also the value seen when the thermistor is always regulated for a complete external temperature variation from -40°C to 85°C. Then the frequency hysteresis due to constraints, $Hys_c(t)$, is:

$$Hys_c(t) = (DF/F_C(t) - DF/F_Cf) / St_Q(t). \quad (7)$$

The effective constraint Hysteresis, Hys_c, is the maximum value seen during the warm-up temperature variation. During a temperature cycling -40°C to 85°C and when the thermistor temperature is regulated, the hysteresis Hys_c is also multiplied by the thermostat gain G_Cf to give Hys_{Fc}. G_Cf and Hys_{Fc} are defined by:

$$G_Cf = DF/F_Cf \ / \ \max(DF/F_C(t)) \ . \quad (8)$$

$$Hys_{Fc} = Hys_c \ . \ G_Cf \ , \quad (9)$$

The total frequency variation, DF/F_F, and the total hysteresis, Hys_F, due to all the components are:

$$DF/F_F = \sum_X DF/F_{Fx} \ , \quad (10)$$

$$Hys_F = \sum_X Hys_{Fx} \ . \quad (11)$$

Using these two results of simulation, the optimization of the design achieved, even in the worst case of the component thermal sensitivity, a very small simulated thermal frequency sensitivity (<9E-9) (Fig.3) and a very small simulated hysteresis (7E-11/°C/min) (Fig.4) in the temperature range -40°C to 85°C. The thermal sensitivity is also reduced, using an internal thermal compensation of a factor 20 (<4.5E-10) (Fig.3). The method of the warm up simulation is simpler, faster and more precise than the simulation of the hysteresis directly during an external temperature cycling from -40°C to 85°C when the thermostat is regulating and when the results are at the limit of the simulator tool.

Component X	Txf (°C)	DTxf (°C)	Gtx	SFx (DF/F /°C)	|DF/F | (-40°C 85°C)	I HysFx I (DF/F/°C/min)
Thermo-mechanics			-3.3E-02	-3.3E-11	1.0E-09	2.0E-11
Xtal	91.71	-0.15	-1.2E-03	5.0E-08	7.5E-09	4.5E-11
Thermistor	91.85	0.00				
Varactor	91.91	0.05	4.1E-04	7.0E-09	3.6E-10	3.0E-12
Inductance	92.16	0.31	2.4E-03	5.6E-10	1.7E-10	2.0E-12
Heater transistor	146.52	54.67				
TOTAL					9.0E-09	7.0E-11
Compensation			5.0E-02		4.5E-10	7.0E-11

Fig. 3. ROD2522S2 10MHz OCXO simulated worst case impact of the critical components to the frequency variation with temperature.

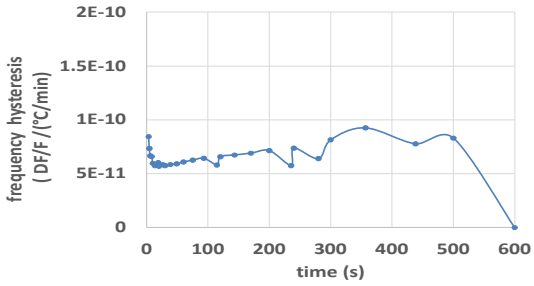

Fig. 4. Total OCXO frequency hysteresis per °C/minute, Hys_F (DF/F per °C/min) deduced from the warm-up simulation and the thermal sensitivity of the critical components.

From the warm up data, we note that the curves are a combination of exponentials:

$$T_X(t) = K_X \left(1 - A_X \ . \ e^{-\left(\frac{t}{\tau_X}\right)} - B_X \ . \ e^{-\left(\frac{t}{\tau_{th}}\right)}\right) P + T_{ext} \ , \quad (12)$$

where τ_{th} is the time constant of the thermistor curve and τ_X is the time delay between the curves of the thermistor and

those of the components X (see τ_{Xtal} for the Xtal on fig. 2). A_X, B_X and K_X are:

$$A_X = \frac{1}{\left(1-\frac{\tau_{th}}{\tau_X}\right)} \text{ and } B_X = \frac{1}{\left(1-\frac{\tau_X}{\tau_{th}}\right)}, \quad (13)$$

$$K_X = \frac{(T_X f - T_{ext})}{P}. \quad (14)$$

The Laplace transfer function of this time dependent fonction is:

$$\frac{T_X(s)}{P(s)} = \frac{K_X}{(1+\tau_X s)(1+\tau_{th} s)}. \quad (15)$$

From these formulations, we extract a simple equivalent thermo-electric model (Fig.5) to simulate electrically the complete thermal loop, taking into account the electrical components, as others had presented methods and results for different designs [3],[4],[5],[6].

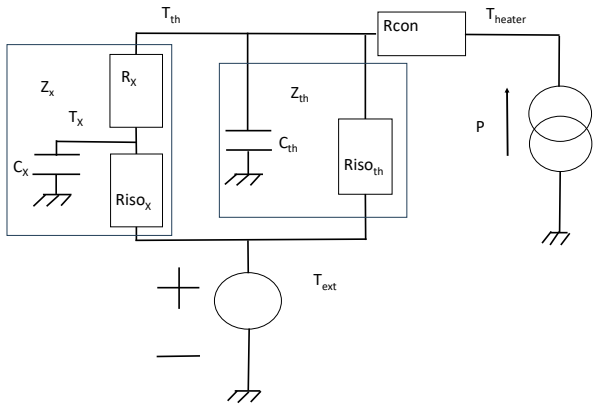

Fig. 5. Thermo-electrical model of the ROD2522S2 thermostat.

In this model, the equivalent Laplace transfer function $T_X(s)/P(s)$ can be simplified as in equation 15, because $Z_{th} << Z_x$. That's what is demonstrated from the warm up curves, with equations 12,13,14 and 15. In that case, the thermal resistances values can be deduced from the final temperatures, the time constants seen on the warm curves and from the specific heat, sh_X, and mass, M_X of the component X:

$$Rcon = \frac{(T_{heater}\, f - T_{th} f)}{P}, \quad (16)$$

$$Riso_{th} = \frac{(T_{th}\, f - T_{ext})}{P}, \quad (17)$$

$$C_{th} = \frac{\tau_{th}}{Riso_{th}}, \quad (18)$$

$$C_X = M_X . sh_X, \quad (19)$$

$$Riso_X = \frac{\tau_X}{C_X . G_X f}, \quad (20)$$

$$R_X = \frac{Riso_X . G_X f}{(1-G_X f)}, \quad (21)$$

$$K_X = \frac{(T_X f - T_{ext})}{P}. \quad (22)$$

Using a SPICE simulator, this model is put in the thermal loop of the thermostat, where the fixed power P source becomes an equivalent controlled current source and the temperature point, T_{Th}, becomes the equivalent voltage used to probe the temperature to stabilize. By adding the electronic components to close the loop, the stability of the thermal loop can be optimized by the adjustment of the electronic components values. Then the impact of the temperature on the consumption, the frequency, the phase noise and the short-term stability, ADEV and TDEV, can be calculated under different conditions: during the warm up (Fig. 6), during a temperature cycling (Fig.7), or in free run (Fig.9, Fig.10 and Fig.11).

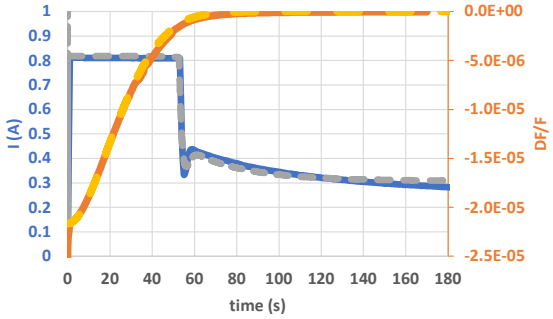

Fig. 6. ROD2522S2 10MHz OCXO during the warm up at Text=25°C: current measurement (blue curve), current simulated curve (dashed gray curve), frequency variation measurement (orange curve), frequency variation measurement (dashed yellow curve).

III. Thermal Sensitivity of the Frequency

The ROD2522S2 frequency versus temperature sensitivity measurement is shown in Fig. 7 and in all physical orientations (X, Y, Z) of the Fig. 1 for the OCXO in the thermal chamber are shown in Fig. 8. In Fig. 7, the hysteresis during a thermal rate of 1°C/min is smaller than 5E-11 and the total frequency variation versus temperature is lower than 1E-10. These results show excellent matching with the simulation results, shown in Fig. 3 and using the simulated model of Fig. 5. The effect of the orientation on the frequency sensitivity to the temperature is lower than 1E-10.

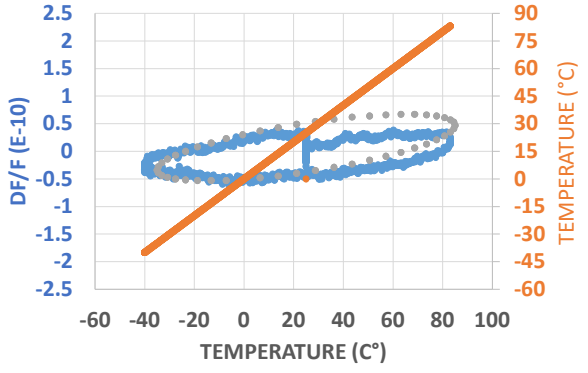

Fig. 7. ROD2522S2 10MHz OCXO temperature sensitivity in -40°C 85°C with a gradient of 1°C/min for the up and down slopes: measurement (blue curve), simulated curve (dashed gray curve).

Axis	DF/F
Z +	6.39E-11
Z -	2.80E-11
Y +	7.90E-11
Y -	1.18E-10
X +	3.69E-11
X -	1.60E-11
min	1.60E-11
Max	1.18E-10

Fig. 8. ROD2522S2 10MHz OCXO frequency versus temperature sensitivity in -40°C 85°C with the 6 orientations of the product in the temperature chamber.

IV. Impact on Phasenoise and Short-Term

The phase noise of the OCXO in PPS DO mode (locked on a UBLOX M8T GNSS receiver pps signal) is shown in Fig. 9. Its short-term curves, locked and in free run, are shown in Fig. 10 in ADEV and in Fig. 11 in TDEV. The noise of the thermal compensation and regulation loop components cause no degradation on the phase noise, the ADEV and TDEV. The time constant, To, of the loop is around two thousand seconds. Below To, the ADEV is mainly due to the OCXO and, above To, is due to the GNSS receiver. Up to a temperature gradient of 10°C/h, there is no impact of the ageing correction loop on the ADEV and TDEV.

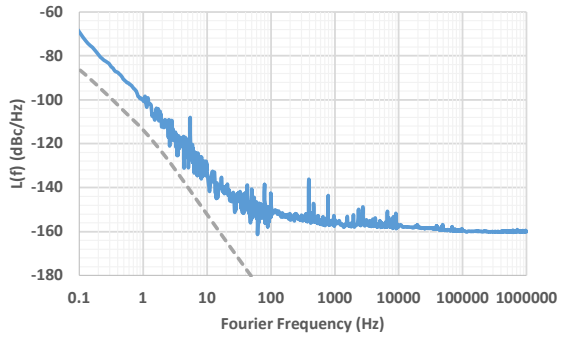

Fig. 9. ROD2522S2 10MHz OCXO Phase noise: measurement (blue curve), thermal loop and compensation noise (dashed grey curve).

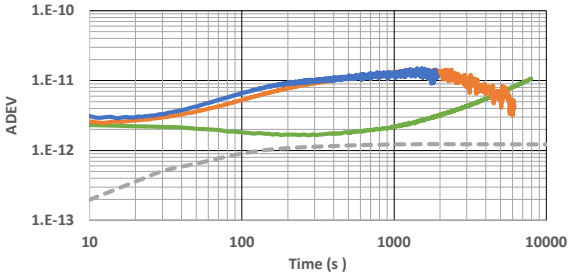

Fig. 10. ROD2522S2 10MHz OCXO measured ADEV: locked on the GNSS receiver pps signal (orange curve), free run (green curve) and with a gradient of 10°C/h (blue curve), thermal loop noise impact (dashed grey curve).

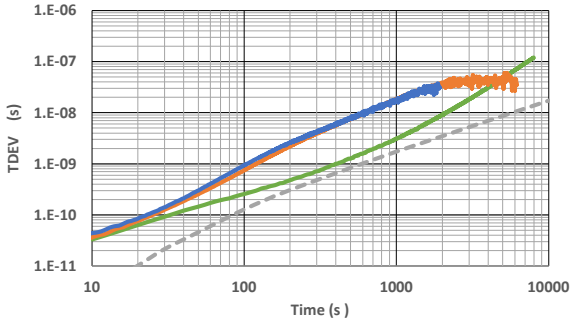

Fig. 11. ROD2522S2 10MHz OCXO measured TDEV: locked on the GNSS receiver pps signal (orange curve), free run (green curve) and with a gradient of 10°C/h (blue curve), thermal loop noise impact (dashed grey curve).

V. Holdover Performance

For the ROD2522S2 platform, two modes of operation are possible for the holdover: the new mode, HV MOD, and the previous mode PPS DO, introduced on the previous platforms [1], [2]. In the new mode HV MOD, the product in always in free run but during the learning phase, it uses the PPS signal of the GNSS receiver to learn its frequency ageing and during the holdover period, it compensates its ageing. Because the Xtal in the ROD2522S2 is the same one used in the previous bigger product,[2], The Xtal ageing of 2E-10/day impacts the holdover performance in the same way and is compatible with the ageing compensation for a holdover of 1.5us over 24h, [1]. The frequency versus temperature sensitivity (DF/F < 5E-10 in -40°C to 85°C) and the hysteresis (Hys_F < 5E-11) performances are also compatible with the holdover of 1.5us over 24h for a step of 4°C of temperature during 24h or with any temperature cycle of 40°C with a gradient of 1°C/min. The holdover performance is shown in Fig. 13 for the HV MOD module and in fig. 12 for 7 parts of 1PPS disciplined OCXO (PPS DO). In these two modes conditions and with a 40 °C cycle variation of temperature and a temperature slope versus time of 1°C/min or with one step of 4°C, the devices have a time interval error less than 1.5us over 24h of holdover.

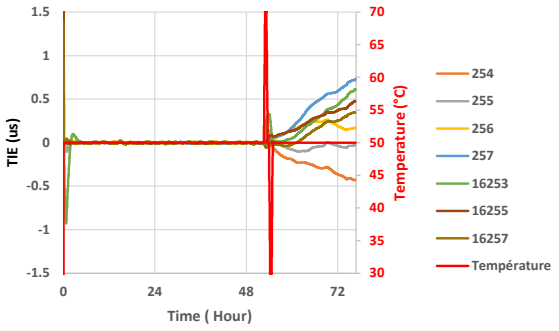

Fig. 12. PPS DO ROD2522S2 10MHz OCXO holdover performance with 52H of locked period and ageing learning followed by 24h of holdover time with +/-20°C variation and a slope of 1°C/min at the beginning of the holdover time on 7 parts.

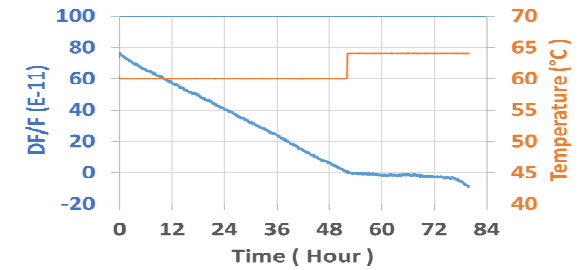

a

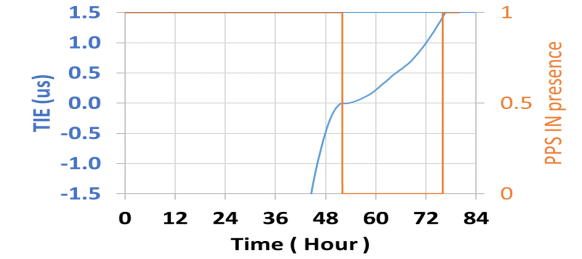

b

Fig. 13. HV MOD ROD2522S2 10MHz OCXO holdover performance with 52h of ageing learning using a GNSS receiver 1pps signal with frequency ageing compensation and a step of +4°C of variation during the 24h of the holdover period: frequency variation (a) and TIE (b).

VI. Conclusion

In conclusion, a method to simulate the thermal performance with respect to OCXO frequency was presented in dynamic and in static states. Utilising a thermo-mechanical finite element simulation of the ROD2522S2 OCXO platform warm up and a RF nonlinear simulation, we had completely defined an equivalent thermo-electrical model of the thermostat and optimized the OCXO structure. By using the same techniques used for the previous bigger platforms, the OCXO thermal response and its ageing compensation were optimized. The thermal performance and the holdover performance, shown in this paper, makes this platform the smallest OCXO that can provide 1.5us holdover over 24h. The ROD2522S2 product, with a patent pending, is now in production. Further developments are in progress to achieve the 1.5us of holdover over 24h without the need of an ageing compensation and with a reduced effect of the thermal hysteresis.

References

[1] J.-C. Billebault, D. Thorax, N. Gufflet, A. Kovach, V. Candelier, H. Henchiri, U. Kumar, F. Vittrant, “Industrial “5G” telecom Infrastructure Time and Frequency Reference”, PTTI 2020.

[2] J.-C. Billebault, D. Thorax, N. Gufflet, A. Kovak, V. Candelier, H. Henchiri, U. Kumar, F. Vittrant, “Next step for delivery of precise frequency and phase OCXO for “5G” telecom and beyond", EFTF IFCS 2021.

[3] R. Brendel, G. Marianneau, F. Djian, and E. Robert, “Improved OCXO’s oven using active thermal insulation,” IEEE Trans. Ultrason., Ferroelectr., Freq. Control, vol. 41, no. 2, pp. 269–274, Mar. 1994.

[4] B. Hillerich and O. Nagler, “Application of finite element method and SPICE simulation for design optimization of oven-controlled crystal oscillators,” IEEE Trans. Ultrason., Ferroelectr., Freq. Control, vol. 48, no. 6, pp. 1662–1668, Nov. 2001

[5] S. Galliou, M. Mourey, F. Marionnet, R. J. Besson, and P. Guillemot, “An oscillator for space,” in Proc. IEEE Int. Freq. Control Symp. PDA Exhib. Jointly, 17th EFTF, Tampa, FL, USA, 2003, pp. 430–434,

[6] L. Xu , P. Ye, S. Liao , C. Chen, and F. Tan, “How Does Ambient Temperature Fluctuation Influence the Short-Term Frequency Stability of OCXO?” IEEE Trans. Ultrason., Ferro-electr, Freq. Control, vol. 70, no. 8, Aug. 2023.

[7] L. Schneller, P. Canzian, V. Candelier, S. Galliou, G. Cibiel "New state of the art of thermal sensitivity with Space Ultra Stable Quartz Crystal Oscillator", *EFTF 2010*.

[8] L. Schneller, S. Galliou, B. Dulmet, P. Canzian, V. Candelier, G. Cibiel, “Effect of Quartz Crystal Thermal Structure on its Performances in Ultra Stable Oscillators” *EFTF 2008*.